

SUPPLEMENTARY MATERIALS

Title: CryoEM and AI reveal a structure of SARS-CoV-2 Nsp2, a multifunctional protein involved in key host processes.

Authors: Meghna Gupta^{1*}, Caleigh M. Azumaya^{1*}, Michelle Moritz^{1*}, Sergei Pourmal^{1*}, Amy Diallo^{1*}, Gregory E. Merz^{1*}, Gwendolyn Jang^{2,3,4,5*}, Mehdi Bouhaddou^{2,3,4,5*}, Andrea Fossati^{2,3,4,5*}, Axel F. Brilot¹, Devan Diwanji¹, Evelyn Hernandez¹, Nadia Herrera¹, Huong T. Kratochvil¹, Victor L. Lam¹, Fei Li¹, Yang Li¹, Henry C. Nguyen¹, Carlos Nowotny¹, Tristan W. Owens¹, Jessica K. Peters¹, Alexandra N. Rizo¹, Ursula Schulze-Gahmen¹, Amber M. Smith¹, Iris D. Young¹, Zanlin Yu¹, Daniel Asarnow¹, Christian Billesbølle¹, Melody G. Campbell^{1,6}, Jen Chen¹, Kuei-Ho Chen^{2,3,4,5}, Un Seng Chio¹, Miles Sasha Dickinson¹, Loan Doan¹, Mingliang Jin¹, Kate Kim¹, Junrui Li¹, Yen-Li Li¹, Edmond Linossi¹, Yanxin Liu¹, Megan Lo¹, Jocelyne Lopez¹, Kyle E. Lopez¹, Adamo Mancino¹, Frank R. Moss III¹, Michael D. Paul¹, Komal Ishwar Pawar¹, Adrian Pelin^{2,3,4,5}, Thomas H. Pospiech Jr.¹, Cristina Puchades¹, Soumya Govinda Remesh¹, Maliheh Safari¹, Kaitlin Schaefer¹, Ming Sun^{1,7}, Mariano C Tabios¹, Aye C. Thwin¹, Erron W. Titus¹, Raphael Trenker¹, Eric Tse¹, Tsz Kin Martin Tsui¹, Feng Wang¹, Kaihua Zhang¹, Yang Zhang¹, Jianhua Zhao¹, Fengbo Zhou¹, Yuan Zhou^{2,3,4,5}, Lorena Zuliani-Alvarez^{1,2,3,4,5}, QCRG Structural Biology Consortium¹, David A Agard^{1,2,3,8}, Yifan Cheng^{1,2,3,8,9}, James S Fraser^{1,2,3,8}, Natalia Jura^{1,2,3,11}, Tanja Kortemme^{1,2,3,10,12}, Aashish Manglik^{1,2,3,13}, Daniel R. Southworth^{1,2,3,8}, Robert M Stroud^{1,2,3,8}, Danielle L Swaney^{2,3,4,5}, Nevan J Krogan^{2,3,4,5,16,&}, Adam Frost^{1,2,3,8,14,&}, Oren S Rosenberg^{1,2,3,8,14,15,&}, Kliment A Verba^{1,2,3,13,&}

Affiliations

¹QBI Coronavirus Research Group Structural Biology Consortium, University of California, San Francisco, CA 94158, USA.

²Quantitative Biosciences Institute (QBI) COVID-19 Research Group (QCRG), San Francisco, CA 94158, USA.

³QBI, University of California, San Francisco, CA 94158, USA.

⁴Department of Cellular and Molecular Pharmacology, University of California, San Francisco, CA 94158, USA.

⁵J. David Gladstone Institutes, San Francisco, CA 94158, USA.

⁶Current affiliation: Division of Basic Sciences, Fred Hutchinson Cancer Research Center, Seattle, WA 98109, USA.

⁷Current affiliation: Beam Therapeutics, Cambridge, MA 02139, USA

⁸Department of Biochemistry and Biophysics, University of California, San Francisco, CA 94158, USA.

⁹Howard Hughes Medical Institute, San Francisco, CA 94158, USA.

¹⁰Department of Bioengineering and Therapeutic Sciences, University of California, San Francisco, CA 94158, USA.

¹¹Cardiovascular Research Institute, University of California, San Francisco, CA 94158, USA.

¹²The University of California, Berkeley–University of California, San Francisco Graduate Program in Bioengineering, University of California, San Francisco, CA 94158, USA.

¹³Department of Pharmaceutical Chemistry, University of California, San Francisco, CA 94158, USA.

¹⁴Chan-Zuckerberg Biohub, San Francisco, CA 94158, USA.

¹⁵Department of Medicine, University of California, San Francisco, CA 94143, USA.

¹⁶Department of Microbiology, Icahn School of Medicine at Mount Sinai, New York, NY 10029, USA.

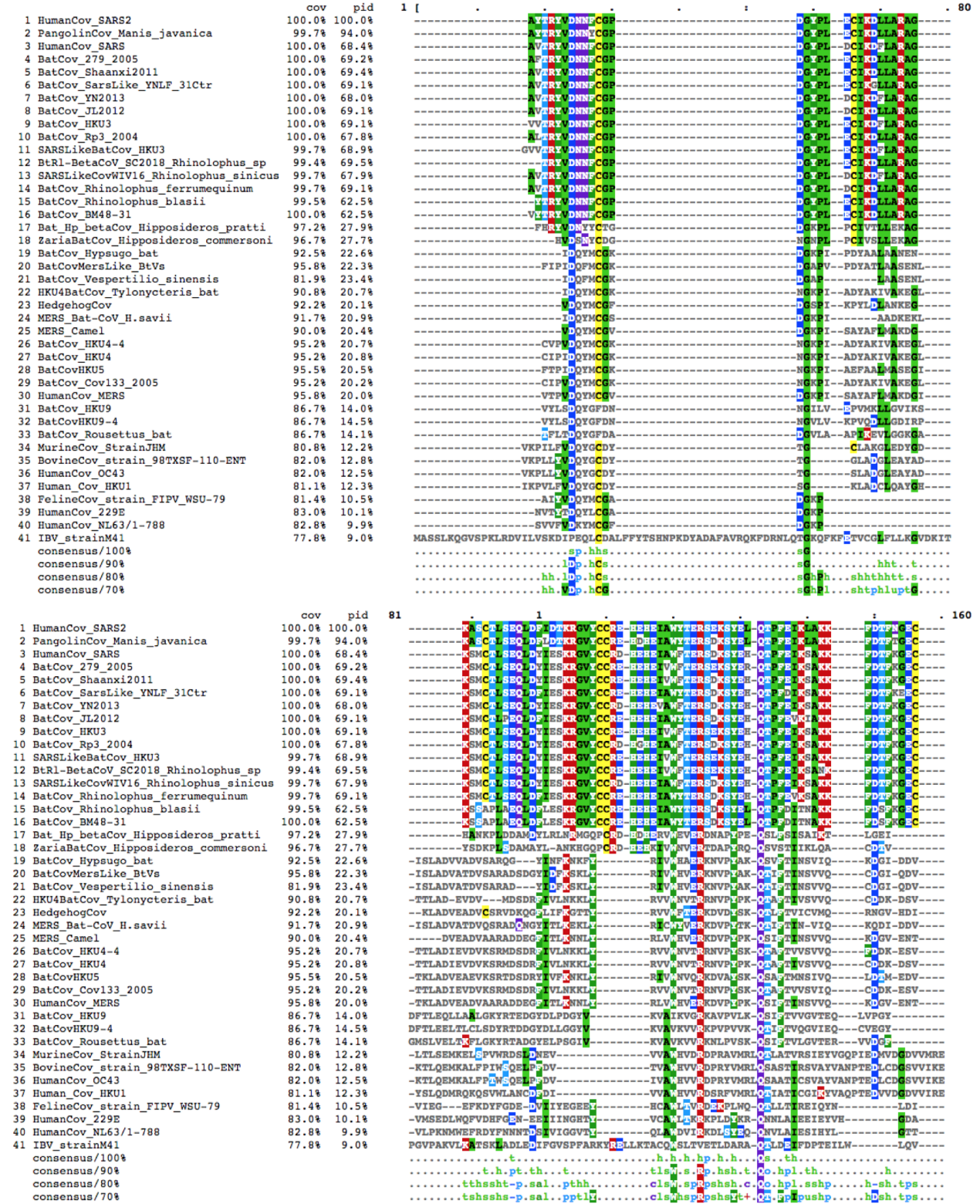
* These authors contributed equally to this work.

& Corresponding authors. A.F., O.S.R. and K.A.V. are corresponding authors on behalf of QCRG Structural Biology Consortium

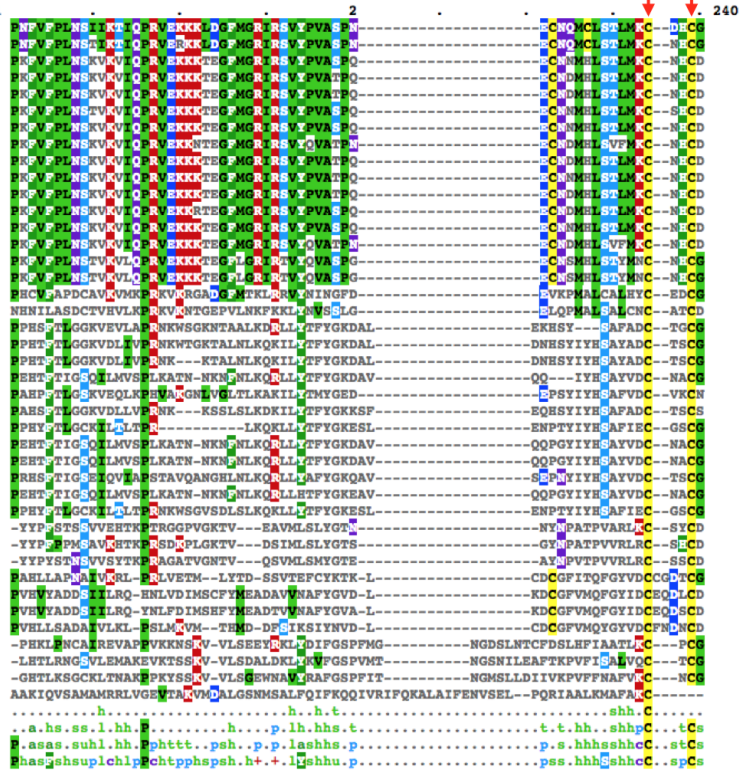
QCRG Structural Biology Consortium Author List

David A. Agard, Daniel Asarnow, Caleigh M. Azumaya, Christian Billesbølle, Axel F. Brilot, David Bulkley, Melody G. Campbell, Jen Chen, Yifan Cheng, Un Seng Chio, Amy Diallo, Miles Sasha Dickinson, Devan Diwanji, Loan Doan, James S. Fraser, Adam Frost, Meghna Gupta, Evelyn Hernandez, Nadia Herrera, Mingliang Jin, Arceli Joves, Almarie Joves, Natalia Jura, Kate Kim, Tanja Kortemme, Huong T. Kratochvil, Victor L. Lam, Fei Li, Yang Li, Junrui Li, Yen-Li Li, Edmond Linossi, Yanxin Liu, Megan Lo, Jocelyne Lopez, Kyle E. Lopez, Adamo Mancino, Aashish Manglik, Liam McKay, Melissa Mendez, Gregory E. Merz, Michelle Moritz, Frank R. Moss III, Henry C. Nguyen, Carlos Nowotny, Tristan W. Owens, Michael D. Paul, Joana Paulino, Komal Ishwar Pawar, Jessica K. Peters, Thomas H. Pospiech Jr., Sergei Pourmal, Cristina Puchades, Soumya Govinda Remesh, Alexandria N. Rizo, Oren S. Rosenberg, Maliheh Safari, Kaitlin Schaefer, Ursula Schulze-Gahmen, Amber M. Smith, Daniel R. Southworth, Robert M. Stroud, Ming Sun, Mariano C. Tabios, Aye C. Thwin, Erron W. Titus, Raphael Trenker, Eric Tse, Tsz Kin Martin Tsui, Kliment A. Verba, Feng Wang, Iris D. Young, Zanlin Yu, Kaihua Zhang, Yang Zhang, Jianhua Zhao, Fengbo Zhou.

Supplementary figure 1. Multiple sequence alignment of Nsp2. Conserved cysteines are marked with red arrows (see positions 230-260 in the alignment).



	cov	pid
1 HumanCov_SARS2	100.0%	100.0%
2 PangolinCov_Manis_javanica	99.7%	94.0%
3 HumanCov_SARS	100.0%	68.4%
4 BatCov_279_2005	100.0%	69.2%
5 BatCov_Shaanxi2011	100.0%	69.4%
6 BatCov_SarsLike_YNLF_31Ctr	100.0%	69.1%
7 BatCov_YN2013	100.0%	68.0%
8 BatCov_JL2012	100.0%	69.1%
9 BatCov_HKU3	100.0%	69.1%
10 BatCov_Rp3_2004	100.0%	67.8%
11 SARSLikeBatCov_HKU3	99.7%	68.9%
12 BtR1-BetaCov_SC2018_Rhinolophus_sp	99.4%	69.5%
13 SARSLikeCovWIV16_Rhinolophus_sinicus	99.7%	67.9%
14 BatCov_Rhinolophus_ferrumequinum	99.7%	69.1%
15 BatCov_Rhinolophus_blasii	99.5%	62.5%
16 BatCov_BM48-31	100.0%	62.5%
17 Bat_Hp_betaCov_Hipposideros_pratti	97.2%	27.9%
18 ZariaBatCov_Hipposideros_commersemi	96.7%	27.7%
19 BatCov_Hypsugo_bat	92.5%	22.6%
20 BatCovMersLike_BtVs	95.8%	22.3%
21 BatCov_Vespertilio_sinensis	81.9%	23.4%
22 HKU4BatCov_Tylonycteris_bat	90.8%	20.7%
23 HedgehogCov	92.2%	20.1%
24 MERS_Bat-CoV_H.savii	91.7%	20.9%
25 MERS_Camel	90.0%	20.4%
26 BatCov_HKU4-4	95.2%	20.7%
27 BatCov_HKU4	95.2%	20.8%
28 BatCovHKU5	95.5%	20.5%
29 BatCov_Cov133_2005	95.2%	20.2%
30 HumanCov_MERS	95.8%	20.0%
31 BatCov_HKU9	86.7%	14.0%
32 BatCovHKU9-4	86.7%	14.5%
33 BatCov_Rousettus_bat	86.7%	14.1%
34 MurineCov_strainJHM	80.8%	12.2%
35 BovineCov_strain_98TXSF-110-ENT	82.0%	12.8%
36 HumanCov_OC43	82.0%	12.5%
37 HumanCov_HKU1	81.1%	12.3%
38 FelineCov_strain_FIPV_WSU-79	81.4%	10.5%
39 HumanCov_229E	83.0%	10.1%
40 HumanCov_NL63/1-788	82.8%	9.9%
41 IBV_strainM41	77.8%	9.0%



	cov	pid
1 HumanCov_SARS2	100.0%	100.0%
2 PangolinCov_Manis_javanica	99.7%	94.0%
3 HumanCov_SARS	100.0%	68.4%
4 BatCov_279_2005	100.0%	69.2%
5 BatCov_Shaanxi2011	100.0%	69.4%
6 BatCov_SarsLike_YNLF_31Ctr	100.0%	69.1%
7 BatCov_YN2013	100.0%	68.0%
8 BatCov_JL2012	100.0%	69.1%
9 BatCov_HKU3	100.0%	69.1%
10 BatCov_Rp3_2004	100.0%	67.8%
11 SARSLikeBatCov_HKU3	99.7%	68.9%
12 BtR1-BetaCov_SC2018_Rhinolophus_sp	99.4%	69.5%
13 SARSLikeCovWIV16_Rhinolophus_sinicus	99.7%	67.9%
14 BatCov_Rhinolophus_ferrumequinum	99.7%	69.1%
15 BatCov_Rhinolophus_blasii	99.5%	62.5%
16 BatCov_BM48-31	100.0%	62.5%
17 Bat_Hp_betaCov_Hipposideros_pratti	97.2%	27.9%
18 ZariaBatCov_Hipposideros_commersemi	96.7%	27.7%
19 BatCov_Hypsugo_bat	92.5%	22.6%
20 BatCovMersLike_BtVs	95.8%	22.3%
21 BatCov_Vespertilio_sinensis	81.9%	23.4%
22 HKU4BatCov_Tylonycteris_bat	90.8%	20.7%
23 HedgehogCov	92.2%	20.1%
24 MERS_Bat-CoV_H.savii	91.7%	20.9%
25 MERS_Camel	90.0%	20.4%
26 BatCov_HKU4-4	95.2%	20.7%
27 BatCov_HKU4	95.2%	20.8%
28 BatCovHKU5	95.5%	20.5%
29 BatCov_Cov133_2005	95.2%	20.2%
30 HumanCov_MERS	95.8%	20.0%
31 BatCov_HKU9	86.7%	14.0%
32 BatCovHKU9-4	86.7%	14.5%
33 BatCov_Rousettus_bat	86.7%	14.1%
34 MurineCov_strainJHM	80.8%	12.2%
35 BovineCov_strain_98TXSF-110-ENT	82.0%	12.8%
36 HumanCov_OC43	82.0%	12.5%
37 HumanCov_HKU1	81.1%	12.3%
38 FelineCov_strain_FIPV_WSU-79	81.4%	10.5%
39 HumanCov_229E	83.0%	10.1%
40 HumanCov_NL63/1-788	82.8%	9.9%
41 IBV_strainM41	77.8%	9.0%



	cov	pid
1 HumanCov_SARS2	100.0%	100.0%
2 PangolinCov_Manis_javanica	99.7%	94.0%
3 HumanCov_SARS	100.0%	68.4%
4 BatCov_279_2005	100.0%	69.2%
5 BatCov_Shaanxi2011	100.0%	69.4%
6 BatCov_SarsLike_YNLF_31Ctr	100.0%	69.1%
7 BatCov_YN2013	100.0%	68.0%
8 BatCov_JL2012	100.0%	69.1%
9 BatCov_HKU3	100.0%	69.1%
10 BatCov_Rp3_2004	100.0%	67.8%
11 SARSLikeBatCov_HKU3	99.7%	68.9%
12 BtR1-BetaCoV_SC2018_Rhinolophus_sp	99.4%	69.5%
13 SARSLikeCovWIV16_Rhinolophus_sinicus	99.7%	67.9%
14 BatCov_Rhinolophus_ferrumequinum	99.7%	69.1%
15 BatCov_Rhinolophus_blasii	99.5%	62.5%
16 BatCov_BM48-31	100.0%	62.5%
17 Bat_Hp_betaCov_Hipposideros_pratti	97.2%	27.9%
18 ZariaBatCov_Hipposideros_commersoni	96.7%	27.7%
19 BatCov_Hypsugo_bat	92.5%	22.6%
20 BatCovMersLike_BtVs	95.8%	22.3%
21 BatCov_Vespertilio_sinensis	81.9%	23.4%
22 HKU4BatCov_Tylosycteris_bat	90.8%	20.7%
23 HedgehogCov	92.2%	20.1%
24 MERS_Bat-CoV_H.savii	91.7%	20.9%
25 MERS_Camel	90.0%	20.4%
26 BatCov_HKU4-4	95.2%	20.7%
27 BatCov_HKU4	95.2%	20.8%
28 BatCovHKU5	95.5%	20.5%
29 BatCov_Cov133_2005	95.2%	20.2%
30 HumanCov_MERS	95.8%	20.0%
31 BatCov_HKU9	86.7%	14.0%
32 BatCovHKU9-4	86.7%	14.5%
33 BatCov_Rousettus_bat	86.7%	14.1%
34 MurineCov_StainJHM	80.8%	12.2%
35 BovineCov_strain_98TXSF-110-ENT	82.0%	12.8%
36 HumanCov_OC43	82.0%	12.5%
37 Human_Cov_HKU1	81.1%	12.3%
38 FelineCov_strain_FIPV_WSU-79	81.4%	10.5%
39 HumanCov_229E	83.0%	10.1%
40 HumanCov_NL63/1-788	82.8%	9.9%
41 IBV_strainM41	77.8%	9.0%
consensus/100%		
consensus/90%		
consensus/80%		
consensus/70%		

```

641          1          7          720
-----
1 HumanCov_SARS2          TSDLVNMLAVMA...          GGVQVTRQW...
2 PangolinCov_Manis_javanica  TSDLVNMLAVMA...          GGVQVTRQW...
3 HumanCov_SARS          TSDLVNMLAVMA...          GGLQOIQW...
4 BatCov_279_2005          TSDLVNMLAVMA...          GGLQOIQW...
5 BatCov_Shaanxi2011          TSDLVNMLAVMA...          GGLQOIQW...
6 BatCov_SarsLike_YNLF_31Ctr  TSDLVNMLAVMA...          GGLQOIQW...
7 BatCov_YN2013          TSDLVNMLAVMA...          GGLQOIQW...
8 BatCov_JL2012          TSDLVNMLAVMA...          GGLQOIQW...
9 BatCov_HKU3          TSDLVNMLAVMA...          GGLQOIQW...
10 BatCov_Rp3_2004          TSDLVNMLAVMA...          GGLQOIQW...
11 SARSLikeBatCov_HKU3          TSDLVNMLAVMA...          GGLQOIQW...
12 BtR1-BetaCoV_SC2018_Rhinolophus_sp  TSDLVNMLAVMA...          GGLQOIQW...
13 SARSLikeCovWIV16_Rhinolophus_sinicus  TSDLVNMLAVMA...          GGLQOIQW...
14 BatCov_Rhinolophus_ferrumequinum  TSDLVNMLAVMA...          GGLQOIQW...
15 BatCov_Rhinolophus_blasii          TSDLVNMLAVMA...          GGLQOIQW...
16 BatCov_BM48-31          TSDLVNMLAVMA...          GGLQOIQW...
17 Bat_Hp_betaCov_Hipposideros_pratti  EYDYS...          INLPIVLD...
18 ZariaBatCov_Hipposideros_commersoni  DNVY...          QNLPVIGD...
19 BatCov_Hypsugo_bat          IGFTAASAYFV...          LHD...
20 BatCovMersLike_BtVs          VGFTAASCFV...          LDEKAEAL...
21 BatCov_Vespertilio_sinensis          VGFTAASCFV...          LDEKAEAL...
22 HKU4BatCov_Tylosycteris_bat          GK...          LDEKFDTV...
23 HedgehogCov          VEISAASMF...          IREKVTM...
24 MERS_Bat-CoV_H.savii          VGFTAASV...          LDEKVES...
25 MERS_Camel          V...          LQ...
26 BatCov_HKU4-4          GK...          LDEKFDTV...
27 BatCov_HKU4          GK...          LDEKFDTV...
28 BatCovHKU5          AV...          LDEKFDTV...
29 BatCov_Cov133_2005          GK...          LDEKFDTV...
30 HumanCov_MERS          V...          LQ...
31 BatCov_HKU9          T...          ATARS...
32 BatCovHKU9-4          Q...          ALTK...
33 BatCov_Rousettus_bat          T...          LAEN...
34 MurineCov_StainJHM          H...          GVA...
35 BovineCov_strain_98TXSF-110-ENT          D...          VDL...
36 HumanCov_OC43          D...          VDL...
37 Human_Cov_HKU1          D...          N...
38 FelineCov_strain_FIPV_WSU-79          D...          V...
39 HumanCov_229E          Y...          L...
40 HumanCov_NL63/1-788          A...          P...
41 IBV_strainM41          A...          I...
consensus/100%          .sth.sts.hhh.h...          .h.phhth...
consensus/90%          .splhssoshhhhh...          .h.phhphsssh...
consensus/80%          .slhssoshhhhh...          .l.pphsphlsl...
consensus/70%

```

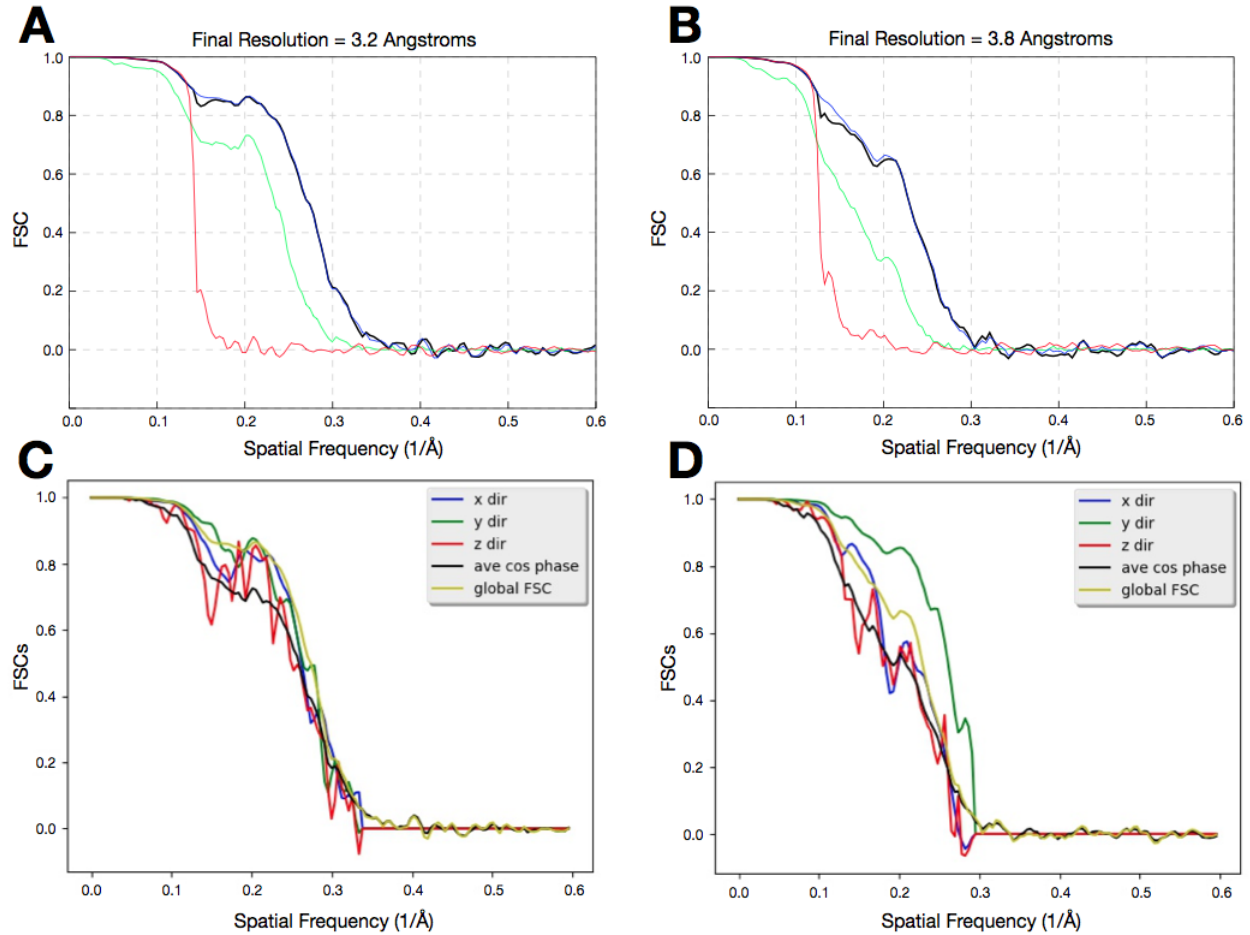
	cov	pid
1 HumanCov_SARS2	100.0%	100.0%
2 PangolinCov_Manis_javanica	99.7%	94.0%
3 HumanCov_SARS	100.0%	68.4%
4 BatCov_279_2005	100.0%	69.2%
5 BatCov_Shaanxi2011	100.0%	69.4%
6 BatCov_SarsLike_YNLF_31Ctr	100.0%	69.1%
7 BatCov_YN2013	100.0%	68.0%
8 BatCov_JL2012	100.0%	69.1%
9 BatCov_HKU3	100.0%	69.1%
10 BatCov_Rp3_2004	100.0%	67.8%
11 SARSLikeBatCov_HKU3	99.7%	68.9%
12 BtR1-BetaCoV_SC2018_Rhinolophus_sp	99.4%	69.5%
13 SARSLikeCovWIV16_Rhinolophus_sinicus	99.7%	67.9%
14 BatCov_Rhinolophus_ferrumequinum	99.7%	69.1%
15 BatCov_Rhinolophus_blasii	99.5%	62.5%
16 BatCov_BM48-31	100.0%	62.5%
17 Bat_Hp_betaCov_Hipposideros_pratti	97.2%	27.9%
18 ZariaBatCov_Hipposideros_commersoni	96.7%	27.7%
19 BatCov_Hypsugo_bat	92.5%	22.6%
20 BatCovMersLike_BtVs	95.8%	22.3%
21 BatCov_Vespertilio_sinensis	81.9%	23.4%
22 HKU4BatCov_Tylosycteris_bat	90.8%	20.7%
23 HedgehogCov	92.2%	20.1%
24 MERS_Bat-CoV_H.savii	91.7%	20.9%
25 MERS_Camel	90.0%	20.4%
26 BatCov_HKU4-4	95.2%	20.7%
27 BatCov_HKU4	95.2%	20.8%
28 BatCovHKU5	95.5%	20.5%
29 BatCov_Cov133_2005	95.2%	20.2%
30 HumanCov_MERS	95.8%	20.0%
31 BatCov_HKU9	86.7%	14.0%
32 BatCovHKU9-4	86.7%	14.5%
33 BatCov_Rousettus_bat	86.7%	14.1%
34 MurineCov_StainJHM	80.8%	12.2%
35 BovineCov_strain_98TXSF-110-ENT	82.0%	12.8%
36 HumanCov_OC43	82.0%	12.5%
37 Human_Cov_HKU1	81.1%	12.3%
38 FelineCov_strain_FIPV_WSU-79	81.4%	10.5%
39 HumanCov_229E	83.0%	10.1%
40 HumanCov_NL63/1-788	82.8%	9.9%
41 IBV_strainM41	77.8%	9.0%
consensus/100%		
consensus/90%		
consensus/80%		
consensus/70%		

```

721          1          800
-----
1 HumanCov_SARS2          F...          ...
2 PangolinCov_Manis_javanica  F...          ...
3 HumanCov_SARS          L...          ...
4 BatCov_279_2005          L...          ...
5 BatCov_Shaanxi2011          L...          ...
6 BatCov_SarsLike_YNLF_31Ctr  L...          ...
7 BatCov_YN2013          L...          ...
8 BatCov_JL2012          L...          ...
9 BatCov_HKU3          L...          ...
10 BatCov_Rp3_2004          L...          ...
11 SARSLikeBatCov_HKU3          L...          ...
12 BtR1-BetaCoV_SC2018_Rhinolophus_sp  L...          ...
13 SARSLikeCovWIV16_Rhinolophus_sinicus  L...          ...
14 BatCov_Rhinolophus_ferrumequinum  L...          ...
15 BatCov_Rhinolophus_blasii          L...          ...
16 BatCov_BM48-31          L...          ...
17 Bat_Hp_betaCov_Hipposideros_pratti  F...          ...
18 ZariaBatCov_Hipposideros_commersoni  F...          ...
19 BatCov_Hypsugo_bat          F...          ...
20 BatCovMersLike_BtVs          F...          ...
21 BatCov_Vespertilio_sinensis  F...          ...
22 HKU4BatCov_Tylosycteris_bat  S...          ...
23 HedgehogCov          P...          ...
24 MERS_Bat-CoV_H.savii          S...          ...
25 MERS_Camel          I...          ...
26 BatCov_HKU4-4          S...          ...
27 BatCov_HKU4          S...          ...
28 BatCovHKU5          S...          ...
29 BatCov_Cov133_2005          S...          ...
30 HumanCov_MERS          I...          ...
31 BatCov_HKU9          A...          ...
32 BatCovHKU9-4          A...          ...
33 BatCov_Rousettus_bat          P...          ...
34 MurineCov_StainJHM          G...          ...
35 BovineCov_strain_98TXSF-110-ENT  G...          ...
36 HumanCov_OC43          G...          ...
37 Human_Cov_HKU1          G...          ...
38 FelineCov_strain_FIPV_WSU-79  D...          ...
39 HumanCov_229E          C...          ...
40 HumanCov_NL63/1-788          A...          ...
41 IBV_strainM41          V...          ...
consensus/100%          .h..hh.t...
consensus/90%          .sh.thh..hhphh.th...
consensus/80%          hsss.ptlt.hhphh.tth...
consensus/70%          hsss.ptlpsphhh.pth...

```

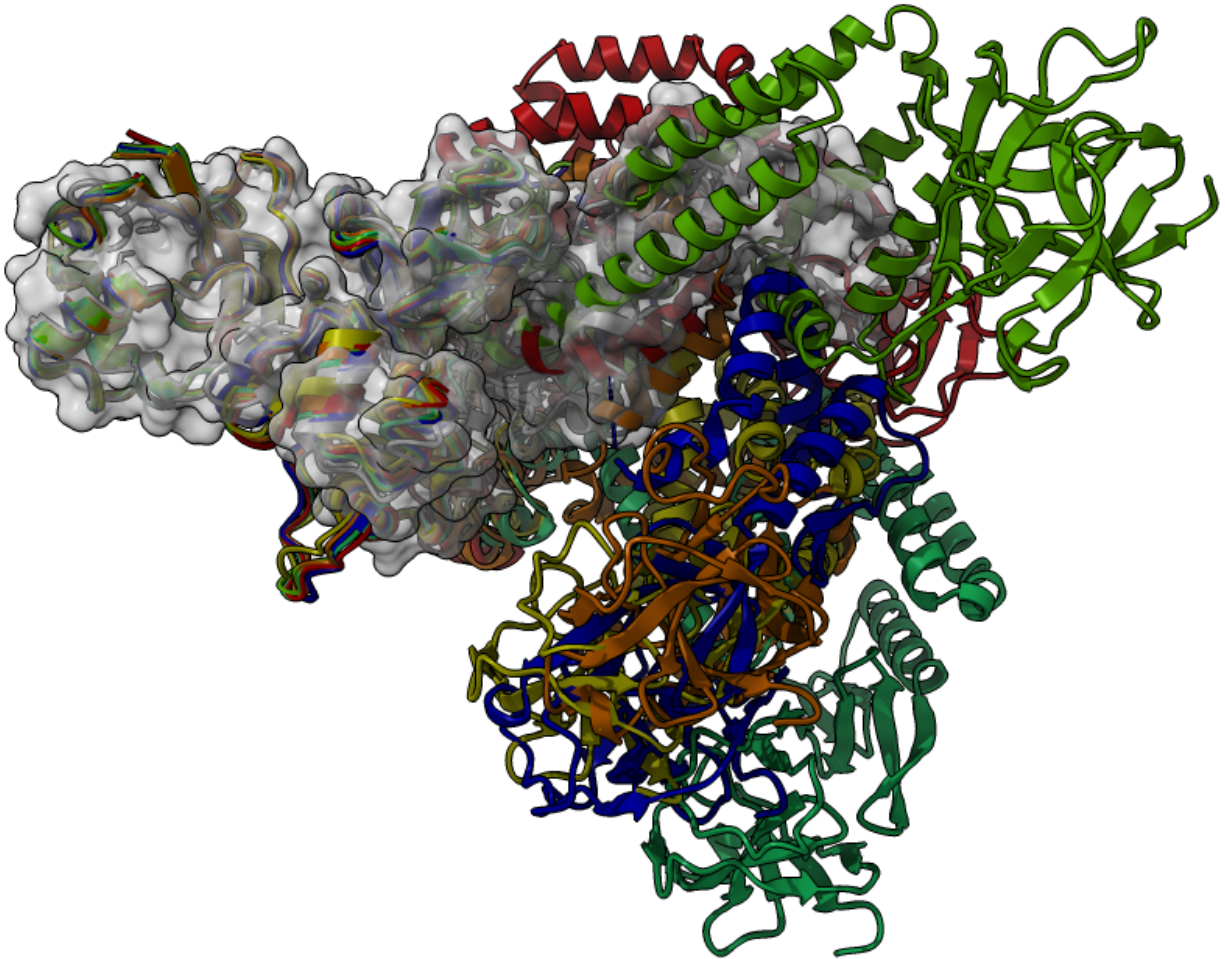

Supplementary Figure 2.



Supplementary Figure 2. Global and directional FSC curves for the Nsp2 cryo-EM reconstructions.

(A) Global FSC curve for the 3.2 Å Nsp2 reconstruction as output from Relion. In black is the final corrected masked FSC. In blue is an uncorrected masked FSC. In green is FSC of unmasked volumes and in red is FSC of the volumes which were phase randomized beyond 7.3 Å. **(B)** Global FSC curve for the 3.8 Å Nsp2 reconstruction as output from Relion. In black is the final corrected masked FSC. In blue is an uncorrected masked FSC. In green is unmasked FSC and in red is FSC of the reconstructions which were phase randomized beyond 8 Å. **(C)** Directional FSC for the 3.2 Å reconstruction of Nsp2 as output by the 3DFSC server, estimated sphericity is 0.86. **(D)** Directional FSC for the 3.8 Å reconstruction of Nsp2 as output by the 3DFSC server, estimated sphericity is 0.81.

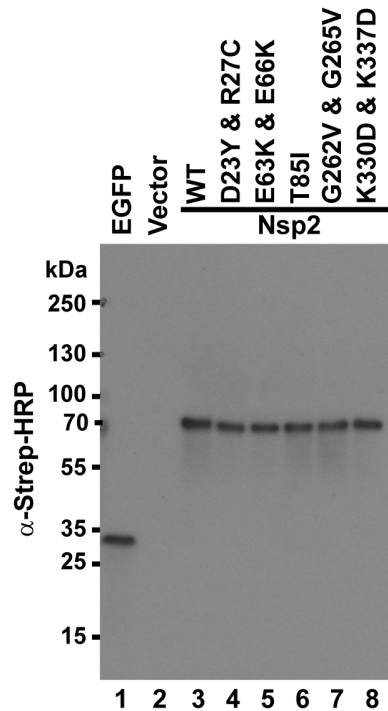
Supplementary Figure 3.



Supplementary Figure 3. AlphaFold2 predictions for Nsp2 have low accuracy in predicting the overall shape of the protein.

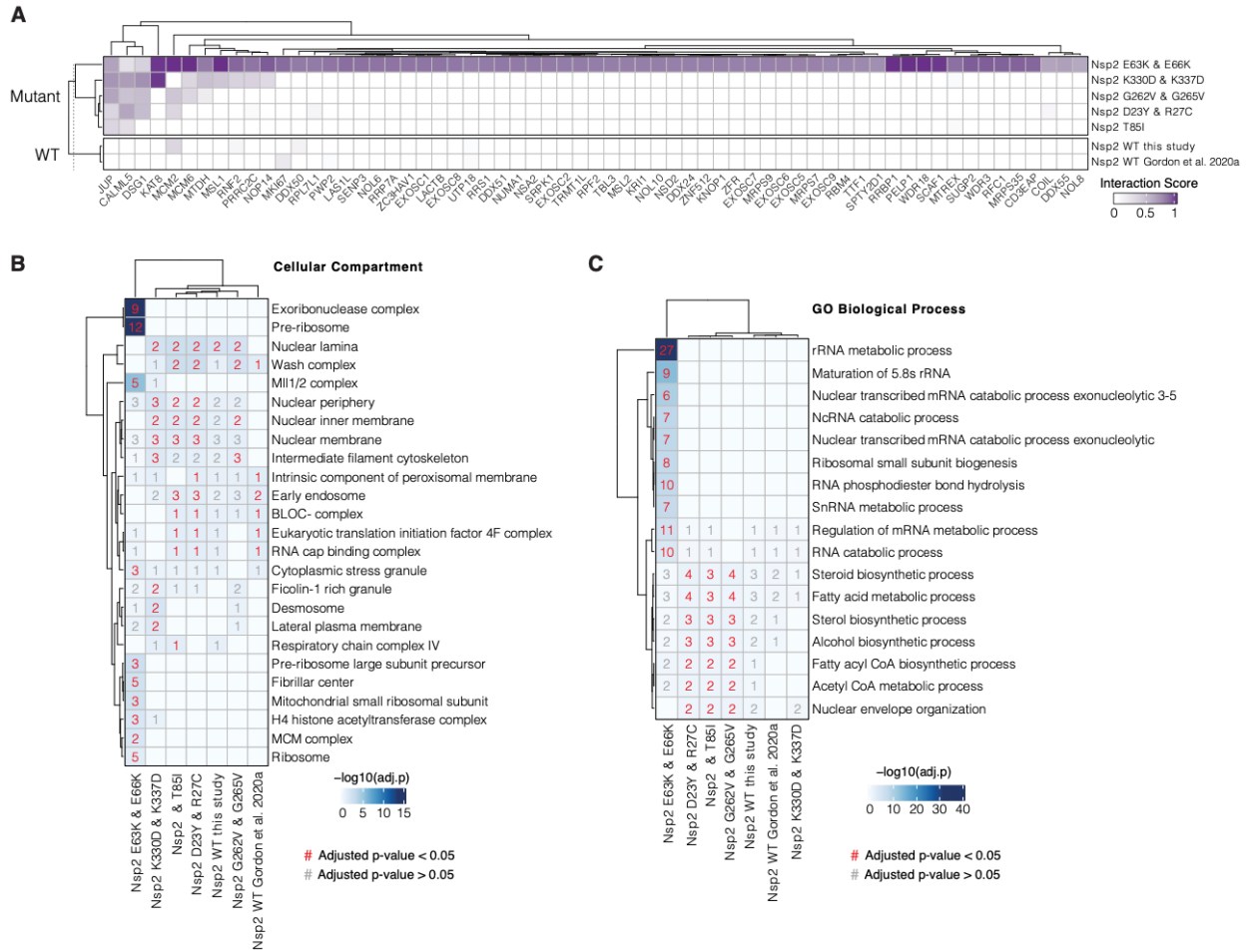
All publicly available predictions from AlphaFold2 team for Nsp2 (multicolored) were aligned to the experimental model of Nsp2 (gray surface). Although individual domains align well locally, globally there is a considerable deviation from the experimental model.

Supplementary figure 4.



Supplementary figure 4. Expression of wild type and mutant SARS-CoV-2 Nsp2 proteins in HEK293T cells. Reserved lysates (50 μ l) were incubated at 95°C for 5 minutes with an equal volume of 2x sample buffer (Morganville Scientific). After further diluting 1:10 in 2x sample buffer, 5 μ l was resolved on a 4-20% Criterion TGX Precast Midi Protein Gel (BioRad) and transferred to a 0.2 mm PVDF membrane using the Trans-Blot Turbo Transfer System (2.5 A, 25 V, 7 minutes). Membranes were blocked with 3% BSA in 1x Phosphate Buffered Saline (PBS) supplemented with 0.2% Tween 20 (0.2% T-PBS) at 4°C and incubated with Strep-Tag II Antibody HRP Conjugate (Millipore) at room temperature for 1 hour (1:10,000 in 1% BSA, 0.2% T-PBS). Membrane was washed in 0.2% T-PBS after blocking and antibody incubation steps and developed with Pierce ECL Western Blotting Substrate (ThermoFisher Scientific).

Supplementary figure 5.



Supplementary figure 5. Nsp2 E63K/E66K Mutation Gains Interactions with Exoribonuclease and Pre-ribosome Components.

(A) Interaction scores (average between MiST and Saint Scores) for human proteins (“preys”) deemed high-confidence interactions in at least one affinity purification (“bait”) mass spectrometry assay and detected to not interact with neither the wild-type Nsp2 in this study or in Gordon et al (2020a). Interaction scores range from zero to one, one being the most high-confidence. **(B)** Gene Ontology Cellular Compartment enrichment analysis (MSigDB) for preys passing the master scoring criteria (see Methods) for each bait (i.e. affinity purification experiment). The top 10 most significant enrichments for each bait are displayed as well as corresponding enrichments for other baits, if applicable. Color denotes the $-\log_{10}$ (adjusted p-value). The number of preys enriched in each bait for each term are shown. Red numbers

indicated adjusted p-values < 0.05 whereas grey numbers indicate adjusted p-values > 0.05 . **(C)**

Same as in B using Gene Ontology Biological Process terms (MSigDB).

Supplementary Table 1. CryoEM collection, refinement and resulting model statistics.

	Nsp2 without Zn (EMDB-xxxx) (PDB xxxx)	Nsp2 with Zn (EMDB-xxxx) (PDB xxxx)
Data collection and processing		
Magnification	105,000x	105,000x
Voltage (kV)	300	300
Electron exposure (e-/Å ²)	66	67
Dose rate (e-/physical pixel/sec)	8	8
Exposure per frame (sec)	0.05	0.05
Defocus range (µm)	-0.8 to -2.4	-0.8 to -2.4
Pixel size (Å)	0.834 (physical)	0.834 (physical)
Symmetry imposed	C1	C1
Initial particle images (no.)	363145+577518	1515264
Final particle images (no.)	42579	81817
Map resolution (Å) FSC threshold	3.76	3.15
Map resolution range (Å)	3.5-6.6	3.0-4.3
Refinement		
Initial model used (PDB code)	ab-initio	ab-initio
Model resolution (Å) FSC threshold 0.143 (Unmasked) FSC threshold 0.5 (Unmasked)	3.6 3.9	3.12 3.46
Model resolution range (Å)	3.6-4.1	3.1-3.5
Map sharpening <i>B</i> factor (Å ²)	-122	-135
Model composition Non-hydrogen atoms Protein residues Ligands	4922 635 Zn: 3	3706 473 Zn: 3
<i>B</i> factors (Å ²) Protein Ligand	194.4 79.8	52.83 50.97

R.M.S. deviations Bond lengths (Å) Bond angles (°)	0.009 0.982	0.008 0.946
Validation MolProbity score Clashscore Poor rotamers (%)	0.86 0.71 0.00	0.75 0.81 0.00
Ramachandran plot Favored (%) Allowed (%) Disallowed (%)	97.31 2.53 0.16	98.07 1.93 0.00